Journal of Sound and Vibration (1998) **215**(3), 439–453
Article No. sv981646

STOCHASTIC MODEL ON A RATTLING SYSTEM

Q. FENG

Department of Mechanics, Tong Ji University, Shanghai, 200092,
People's Republic of China

AND

F. PFEIFFER

Institute for Mechanics B, Technical University Munich, Arcistrasse 21, *D*-80335 *Munich*,
Germany

(*Received* 10 *March* 1997, *and in final form* 10 *March* 1998)

Rattling in change-over gears of automobiles is an unwanted comfort problem. In recent years very general models have been developed to analyze the rattling phenomenon. One of them, in consideration of plays being the consequence of tolerances, of backlashes and others, is modelled as an impulsive system that consists of some gears not under load being able to rattle. Modern research has shown that chaotic vibration can occur on impulsive systems with plays, which are confident of a non-linear element in mechanics. Therefore, the chaotic vibration on a rattling system has received attention. In this paper, instead of performing the very tedious numerical calculation for a rattling system, a discrete stochastic model described by a mean map is established using the non-Gaussian closure technique. By the analysis of the example this model can reveal chaotic stochastic behaviour. Based on a detailed investigation the existence of random chaos can be justified. This finding in a special impulsive system is also significant for chaos study.

1. INTRODUCTION

Rattling in change-over gears of automobiles is an unwanted comfort problem. In recent years very general models have been developed to analyze the rattling phenomenon [1–4]. One of them, in consideration of plays being the consequence of tolerances, of backlashes and others, is modelled as an impulsive system that consists of some gears not under load being able to rattle [5]. Modern research has shown that chaotic vibration can occur on impulsive systems with plays, which are confident of a non-linear element in mechanics [6]. Therefore, the chaotic vibration on a rattling system has received attention.

In 1988, Pfeiffer came up with an idea from Fermi's experiment and elaborated a discrete model using a map to describe the rattling vibration [5]. By means of experiment and numerical simulation, a detailed analysis was performed by Karagiannis and Kunert [7–11]. A significant step was taken by Pfeiffer and Kunert, who considered the effects of an additional noise and introduced stochastic modelling into the analysis [9]. The random model is also more realistic because a finite level of noise is present everywhere in reality. However, their analysis was only limited to the investigation of the deterministic chaos using the stochastic perturbing technique. In fact, due to influence of the noise, another type of vibration can be induced. On the one hand, except for an additional noise, a random modulation of the control parameter of a non-linear system can also induce interesting behaviour [12], and on the other hand, chaotic stochastic vibration may occur

0022–460X/98/330439 + 15 $30.00/0

in random dynamical systems [13]. In the present paper, these problems are considered in detail.

The concept of the chaotic stochastic vibration was proposed by Kapitaniak in 1988 [13]. He interpreted that for a random dynamical system, the chaotic behaviour of statistical results including mean value and probability density indicates a new motion called chaotic stochastic vibration. Kapitaniak's work was based on the average results of finite performances of the numerical simulation for an unstable Duffing's oscillator. In this paper, instead of performing the very tedious numerical calculation for a rattling system, a discrete stochastic model described by a mean map is established using the non-Gaussian closure technique. By means of the analysis of the example it is proved that the model can reveal chaotic stochastic behaviour. Through investigation, the *Poincaré* maps exhibit typical chaotic vibrations and the power spectrum of mean velocity shows characteristics of a continuous spectrum. Moreover, it is discovered that the time difference of two successive impacts is a white noise process. The results again demonstrate the existence of the chaotic stochastic vibration. The routes to random chaos in the frequency domain display more complexity compared with one for deterministic chaos. The findings in a special impulsive system are also significant for chaos study.

2. DISCRETE STOCHASTIC MODEL

Due to unbalance of the engine small and mostly harmonic vibrations enter the gear-box and excite all gears. In that case, two different phenomena, rattling and hammering, may occur depending on the exciting torque. In the following, attention is focused on the first one. In change speed gears, for example, it is discovered that some gear wheels not under load are able to rattle. In this case, the teeth of the gear wheels come into contact only for a very short time, where contact moment is small. An impulsive process of this type can be approximated very well by a generalized impact theory. The basic idea is simple. Consider a shift transmission with many plays and assume that in one of these plays an impact has just taken place so that one starts with free flight phase in the various plays. Contact in one of the plays is indicated by zero relative distances. For that system, one must evaluate the backlash where a contact occurs at the earliest. Then one can apply a generalized impact theory yielding the state shortly after that impact, which serves as the initial state for the next free flight phase. The results of such a patching method depend very much on the accuracy of interpolating the impulsive events. Based on that argument, a discrete model on deterministic rattling vibration has been obtained [5].

A random description may be fitting for the properties of the real world, because even with modern production possibilities no gear tooth can be manufactured in an ideal way and there is a lot of additional small irregularities due to oil splash and the complete system behaviour. Therefore, in reference [9], an appropriate description is given by a probability distribution for the state space. In the free flight phase, the dynamical system is then described by a corresponding Fokker–Planck equation. The boundary conditions for the probability density are derived from the classical impact theory. Using finite differencing methods, the solution of F–P equation with the probability boundaries can be approximated. However, performance of finite differential methods takes a lot of time on the computer, which is very uneconomical and inconvenient. Moreover, in reference [8], it has been shown that rattling noise in real gear-boxes does not depend in a significant way on the structural properties of the corresponding non-linear vibrations; it depends mainly on the parameter influencing the mean values of the impulsive processes. Therefore, a more adequate description by mean value on the random rattling system will need to evolve.

2.1. MECHANICAL MODEL

To develop a stochastic model, a brief review about the deterministic model is necessary. In this paper, only a single stage rattling system is considered. In Figure 1, the driven gear wheel not under load can move freely between backlashes, and the free flight motion is only stopped by the backlash boundary, where an impact occurs. According to what has been mentioned above, the motion of the driven wheel can be distinguished into two phases: the free flight phase and the contact phase. The motion equation can be written in the following way:

$$I_1\ddot{\phi}_1 + d_1\dot{\phi}_1 = -T_1, \tag{1}$$

for the free flight phase and the contact phase is expressed by

$$\dot{\phi}_1^+ = -\varepsilon\dot{\phi}_1^- + (1+\varepsilon)\frac{R_e}{R_1}\dot{e}(t), \tag{2}$$

in which R_e and R_1 are basic radii; $e(t)$ is a harmonic rotation with amplitude a and frequency ω; v_1 indicates a constant play in mesh plane; I_1 stands for inertia moment of driven gear wheel; ϕ_1 is angular displacement; T_1 denotes a constant moment; d_1 means damping ratio in free flight phase; and ε is the restitution coefficient. The signs $(-)$ and $(+)$ denote short time before and after impact. During the infinitesimal short impact all position and orientation magnitudes remain unchanged.

First, the above motion equation is reformed to be described by relative displacement and relative velocity. If

$$\tau = \omega t, \qquad x = \frac{R_e e(t) - R_1\phi_1}{v_1}, \qquad \beta = \frac{d_1}{I\omega}, \qquad \gamma = \frac{T_1 R_1}{I v_1 \omega^2}, \qquad \alpha = \frac{R_e a}{v_1},$$

the following dimensionless equations are obtained:

$$\begin{cases} \dot{x} = y, \\ \dot{y} = -\beta y + \gamma + \ddot{f} + \beta\dot{f}, \end{cases} \tag{3}$$

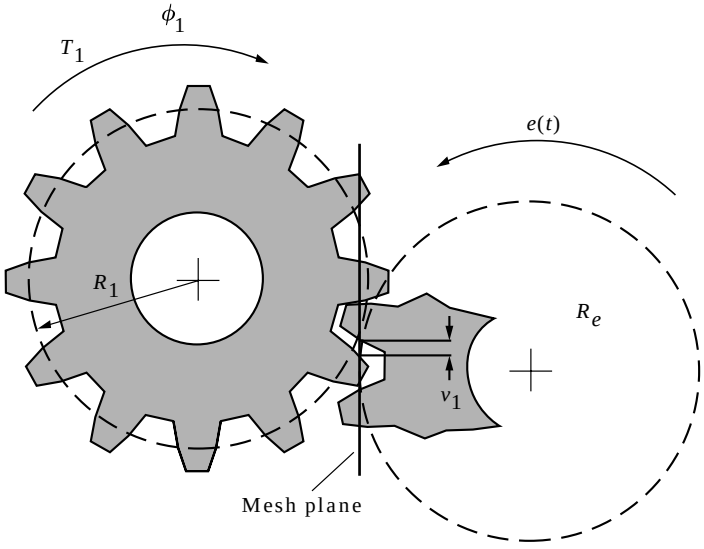

Figure 1. Mechanical model.

in the free flight phase, $x \in (-0{\cdot}5, 0{\cdot}5)$ and

$$y^+ = -\varepsilon y^-, \tag{4}$$

in the contact phase, $x \in (-0{\cdot}5, 0{\cdot}5)$, where x and y are relative displacement and relative velocity, respectively. β is the damping ratio in the free flight phase, γ indicates constant moment, $f(\tau) = \alpha \sin \tau$, τ is dimensionless time, and α stands for excitation amplitude. For the above equations, patching and point mapping equations are particularly simple. An accurate solution by a map for the above deterministic equations has been derived [11].

In the prsent paper, a stochastic model is considered. Considering a general case, the excitation function is perturbed by an addition noise and a modulation noise. It is assumed that the magnitude of backlash consists of two parts: average value and measure tolerance. After normalizing, the backlash magnitude is equal to $1 + 2d$, where d is a stochastic variable with null mean value whose maximum value is d_m. Then a modified motion equation can be written as:

$$\begin{cases} \dot{x}_\sigma = y_\sigma, \\ \dot{y}_\sigma = -\beta y_\sigma + \gamma + \sigma_1 \eta(\tau) + [\alpha + \sigma_2 \eta(\tau)][\sin \tau + \beta \cos \tau], \end{cases} \tag{5}$$

in the free flight phase, $x_\sigma \in (-(0{\cdot}5 + d), (0{\cdot}5 + d))$. The subscript σ indicates a perturbed system that differs from unperturbed systems (3) and (4), x_σ and y_σ describe the dimensionless relative displacement and velocity of a perturbed system and α is the deterministic part of the excitation amplitude. All other parameters are the same as in equation (3). $\sigma_i (i = 1, 2)$ represents the intensity of random forces described by a standard Gaussian white noise $\eta(\tau)$. It satisfied the following conditions.

$$E[\eta(\tau)] = 0 \qquad \text{and} \qquad E[\eta(\tau)\eta(s)] = \delta(\tau - s).$$

According to the classical impact theory, in the contact phase, $x_\sigma \in \{-(0{\cdot}5 + d), (0{\cdot}5 + d)\}$, it has

$$y_\sigma^+ = -\varepsilon y_\sigma^- . \tag{6}$$

2.2. DISCRETE MODEL

In general, when noise intensity is small, the stochastic models (5) and (6) can be considered as a modification for the determinsitc models (3) and (4). Equation (5) is a non-linear equation without a high order term that can be decoupled. To derive a discrete model, it is attempted to decouple equations (5) and (6) into two parts: deterministic and stochastic. Because the modification value of the backlash d is very small, in the following derivation the influence of d is not considered. First, it is assumed that the solution of perturbed systems (5) and (6) can be separated into deterministic and stochastic parts with the form

$$\begin{cases} x_\sigma = x + \xi \\ y_\sigma = y + \xi \end{cases}, \tag{7}$$

in which x and y are solutions of unperturbed systems (3) and (4), while ξ and ζ are stochastic variables. Substituting equation (7) into equations (5) and (6), and subtracting equations (3) and (4), respectively, one obtains

$$\begin{cases} \dot{\xi} = \zeta \\ \dot{\zeta} = -\beta\zeta + \{\sigma_1 + \sigma_2[\sin \tau + \beta \cos \tau]\}\eta(\tau), \end{cases} \tag{8}$$

in the free flight phase, $\xi \in (-(0{\cdot}5 + d + x), (0{\cdot}5 + d) - x)$ and

$$\zeta^+ = -\varepsilon\zeta^-. \tag{9}$$

in the contact phase, $\xi \in \{-(0{\cdot}5 + d + x), (0{\cdot}5 + d) - x\}$.

Now equations (5) and (6) have been separated into two parts. The deterministic part is the same as equations (3) and (4). The stochastic part consists of equations (8) and (9). The solution of the deterministic part can be obtaind by use of the patching method, as in references [5, 11]. Integrating equation (3), if the sequence of system states before or after impacts are known, x and y can be defined exactly. Considering the mapping before impact H: $\mathbf{X}_k^- \to \mathbf{X}_{k+1}^-$, in which $\mathbf{X} = [x, y]^T$ is a state vector of the unperturbed system, an iterated operator (10) is obtained as derived in reference [11],

$$\begin{aligned} x_{k+1}^- &= x_k^- + \alpha(\sin\tau_{k+1} - \sin\tau_k) \\ &\quad + \frac{1}{\beta}(1 - \exp(-\beta\Delta\tau_k))\left(-\varepsilon y_k^- - \alpha\cos\tau_k - \frac{\gamma}{\beta}\right) + \frac{\gamma}{\beta}\Delta\tau_k, \\ y_{k+1}^- &= \alpha\cos\tau_{k+1} + \left(-\varepsilon y_k^- - \alpha\cos\tau_k - \frac{\gamma}{\beta}\right)\exp(-\beta\Delta\tau_k) + \frac{\gamma}{\beta}. \end{aligned} \tag{10}$$

In the above operator, the time difference $\Delta\tau_k$ of the two successive impacts has not been defined yet. Now look at the stochastic part. Equation (8) in the free flight phase is a non-linear stochastic differential equation whose exact solution cannot be solved. Because there is no restitution force term in equation (8), the correlation coefficient ρ of the random variables ξ and ζ from the corresponding moment equation of equation (8) does not always satisfy the relation $\rho \leqslant 1$ and, therefore, its distribution is out of accordance with a Gaussian normal distribution. To derive a mean iterated operator analytically, a non-Gaussian closure technique is used here. An Edgeworth expansion in reference [14] is adopted to approximate the true distribution. The two-dimensional Edgeworth expansion is expressed as

$$\begin{aligned} P^*(\xi,\zeta) &= P(\xi,\zeta)\left\{\sum_{k=0}^{N}\frac{\rho^k}{k!}H_k\left(\frac{\xi}{\sigma_\xi}\right)H_k\left(\frac{\zeta}{\sigma_\zeta}\right)\right. \\ &\quad + \sum_{j+l=3}^{N}\frac{1}{j!l!}\frac{\lambda_{jl}}{\sigma_\xi^j\sigma_\zeta^l}\sum_{k=0}^{N}\frac{\rho^k}{k!}H_{k+j}\left(\frac{\xi}{\sigma_\xi}\right)H_{k+l}\left(\frac{\zeta}{\sigma_\zeta}\right) \\ &\quad + \sum_{j+l=4}^{N}\frac{1}{j!l!}\frac{\lambda_{jl}}{\sigma_\xi^j\sigma_\zeta^l}\sum_{k=0}^{N}\frac{\rho^k}{k!}H_{k+j}\left(\frac{\xi}{\sigma_\xi}\right)H_{k+l}\left(\frac{\zeta}{\sigma_\zeta}\right) \\ &\quad \left. + \frac{1}{2}\sum_{j+l=3,r+s=4}^{N}\frac{1}{j!l!r!s!}\frac{\lambda_{jl}}{\sigma_\xi^j\sigma_\zeta^l}\frac{\lambda_{rs}}{\sigma^r\sigma_\zeta^s}\sum_{k=0}^{N}\frac{\rho^k}{k!}H_{k+j+r}\left(\frac{\xi}{\sigma_\xi}\right)H_{k+l+s}\left(\frac{\zeta}{\sigma_\xi}\right)\right), \end{aligned} \tag{11}$$

where moments $\lambda_{np} = E[\xi^n\ \zeta^p]$, $(n = j\ \text{or}\ r, p = l\ \text{or}\ s)$ and the correlation $\rho = \lambda_{11}/\sigma_\xi\sigma_\zeta$. The polynomial $H_k(z)$ is in the form of reference [14],

$$H_0(z) = 1, H_1(z) = z, H_2(z) = z^2 - 1, \qquad H_3(z) = z^3 - 3z, H_4(z) = z^4 - 6z^2 + 3, \ldots$$

in which $P(\xi, \zeta)$ means a standard Gaussian normal distribution. It has the form of

$$P(\xi, \zeta) = \frac{1}{2\pi\sigma_\xi\sigma_\zeta} \exp\left(-\frac{(\xi - m_\xi)^2}{2\sigma_\xi^2}\right) \exp\left(-\frac{(\zeta - m_\zeta)^2}{2\sigma_\zeta^2}\right), \tag{12}$$

where the standard derivations $\sigma_i (i = \xi, \zeta)$ and the mean values $m_i (i = \xi, \zeta)$ can be solved from the 2-order and the 1-order moment equations, respectively.

It seems probable that the distribution (10) obtained by the method of non-Gaussian closure will eventually converge to that of the true distributions as $N \to \infty$. In the process, the accuracy of approximation for most statistics constructed from the distribution will generally improve as N increases. It is, however, possible for some particular statistics on some oscillators to suffer a decrease in accuracy when at some stage N is increased to $N + 2$ [15]. That is a defect of non-Gaussian closure technique. However, in the problem under consideration, this defect can be avoided. The reason may be interpreted in the following. The approximated accuracy of the distribution $P^*(\xi, \zeta)$ is determined by λ_{np} which can be solved from a set of corresponding moment equations. For example, in reference [15] there are higher order terms in equations, so the moment equation chains are not closed. After closing, the accuracy of moments cannot be warranted. In our problem, moments λ_{np} can be determined from the following:

$$\begin{aligned}
\dot{\lambda}_{np} &= \frac{\partial E[\xi^n\zeta^p]}{\partial\tau} \\
&= E\left[\zeta\frac{\partial(\xi^n\zeta^p)}{\partial\xi}\right] - \beta E\left[\zeta\frac{\partial(\xi^n\zeta^p)}{\partial\zeta}\right] + \frac{\chi(\tau)}{2} E\left[\frac{\partial^2(\xi^n\zeta^p)}{\partial\zeta^2}\right], \\
\chi(\tau) &= [\sigma_1 + \sigma_2(\sin\tau + \beta\cos\tau)]^2, \qquad (n, p = 0, 1, 2, \ldots)
\end{aligned} \tag{13}$$

in the free flight phase. In the contact phase, there exists the impact constrained conditions of the moments as

$$\begin{cases} \lambda_{np}^+ = -\varepsilon\lambda_{np}^- & \text{if} \quad p \neq 0 \\ \lambda_{np}^+ = \lambda_{np}^- & \qquad\ \ p = 0 \end{cases} \qquad (n, p = 0, 1, 2, \ldots) \tag{14}$$

In the free flight phase, the moment equation chains (13) are closed and the moments can be solved uniquely without closing tolerance. Therefore, the approximated distribution can tend to the true one, if $N \to \infty$. Integrating equation (13), all moments in the time interval $\Delta\tau_k$ can be obtained when initial moments from equation (14) are known. Considering the mapping before impact $H_\sigma: [\lambda_{np}]_k^- \to [\lambda_{np}]_{k+1}^-$, a set of iterated operators for all moments is obtained. Introducing the initial conditions $[\lambda_{np}]_0 = 0$, all odd order moments are equal to zero, and a set of iterated operators of all even order moments are derived as follows.

Case 1, $\sigma_1 \neq 0$, $\sigma_2 = 0$:

$$[\lambda_{02}]_{k+1}^- = \left\{-\varepsilon[\lambda_{02}]_k^- - \frac{\sigma_1^2}{2\beta}\right\} \exp(-2\beta\Delta\tau_k) + \frac{\sigma_1^2}{2\beta}$$

$$[\lambda_{11}]_{k+1}^- = -\left\{\varepsilon[\lambda_{11}]_k^- + \frac{\varepsilon}{\beta}[\lambda_{02}]_k^- + \frac{\sigma_1^2}{\beta^2}\right\} \exp(-\beta\Delta\tau_k) + \left\{\frac{\varepsilon}{\beta}[\lambda_{02}]_k^- + \frac{\sigma_1^2}{2\beta^2}\right\} \exp$$

$$\times(-2\beta\Delta\tau_k) + \frac{\sigma_1^2}{2\beta^2},$$

$$[\lambda_{20}]_{k+1}^- = \frac{1}{\beta}\left\{\varepsilon[\lambda_{11}]_k^- + \frac{\varepsilon}{\beta}[\lambda_{02}]_k^- + \frac{\sigma_1^2}{\beta^2}\right\} \exp(-\beta\Delta\tau_k) - \frac{1}{2\beta}\left\{\frac{\varepsilon}{\beta}[\lambda_{02}]_k^- + \frac{\sigma_1^2}{2\beta^2}\right\} \exp$$

$$\times(-2\beta\Delta\tau_k) + \frac{\sigma_1^2}{2\beta^2}\Delta\tau_k,$$

. . . . .

Case 2, $\sigma_1 = 0$, $\sigma_2 \neq 0$:

$$[\lambda_{02}]_{k+1}^- = a_2 \exp(-2\beta\Delta\tau_k) + a_0 + a_{01} \sin 2\tau_{k+1} + a_{02} \cos 2\tau_{k+1},$$

$$[\lambda_{11}]_{k+1}^- = b_1 \exp(-\beta\Delta\tau_k) + b_2 \exp(-2\beta\Delta\tau_k) + b_0 + b_{01} \sin 2\tau_{k+1} + b_{02} \cos 2\tau_{k+1},$$

$$[\lambda_{20}]_{k+1}^- = -\frac{2b_1}{\beta} \exp(-\beta\Delta\tau_k) - \frac{b_2}{\beta} \exp(-2\beta\Delta\tau_k) + 2b_0\tau_k + b_{02} \sin 2\tau_{k+1}$$

$$+ b_{01} \cos 2\tau_{k+1},$$

. . . . ,

where

$$a_2 = -\left\{\varepsilon[\lambda_{02}]_k^- + \frac{\sigma_2^2(1+\beta^2)}{2\beta} + \frac{\sigma_2^2}{2} \sin 2(\tau_k + \alpha_0)\right\},$$

$$a_0 = \frac{\sigma_2^2(1+\beta^2)}{2\beta}, \qquad a_{01} = \frac{\sigma_2^2}{2} \cos 2\alpha_0, \quad a_{02} = \frac{\sigma_2^2}{2} \sin 2\alpha_0,$$

$$b_2 = \frac{a_2}{\beta}, \qquad b_0 = \frac{a_0}{\beta}, \qquad b_{01} = \frac{2a_{02} + \beta a_{01}}{4+\beta^2}, \qquad b_{02} = \frac{2a_{02} - \beta a_{01}}{4+\beta^2},$$

$$b_1 = -\{\varepsilon[\lambda_{11}]_k^- + b_2 + b_0 + b_{01} \sin 2\tau_k + b_{02} \cos 2\tau_k\},$$

$$\alpha_0 = \operatorname{arctg}(-\beta),$$

. . . . .

To derive the iterated operator of stochastic parts, it is assumed that the probability distribution of the system between the two successive impacts can be approached by equation (11) and it can be deduced from equation (15) for the state before impact.

$$P_{k+1}^*(\xi, \zeta) = P(\xi, \zeta) \sum_{i=0}^{N} \sum_{j=0}^{N} [a_{ij}]_{k+1}^- H_i\left(\frac{\xi}{[\sigma_\xi]_k}\right) H_j\left(\frac{\zeta}{[\sigma_\zeta]_k}\right), \tag{15}$$

where the coefficients $[a_{ij}]_{k+1}^-$ are the functions related to moments $[\lambda_{np}]_{k+1}^-$ and can be derived from equation (11).

$$[a_{01}]_{k+1}^- = 0, \qquad [a_{11}]_{k+1}^- = \frac{[\lambda_{11}]_{k+1}^-}{[\sigma_\xi][\sigma_\xi]} = [\rho_{\xi\zeta}]_{k+1}^-, \qquad \ldots\ldots$$

After two integrations of equation (15), the discrete mean values of random variables ξ and ζ for the states before impact are expressed as follows

$$\begin{aligned} E[\xi]_{k+1}^- &= \int_{-(0{\cdot}5 + d_m + x)}^{(0{\cdot}5 + a_m) - x} \xi \int_{-\infty}^{\infty} P_{k+1}^*(\xi, \zeta)\, \mathrm{d}\zeta\, \mathrm{d}\xi \\ &= [\sigma_\xi]_k A_{k+1}^-, \\ E[\zeta]_{k+1}^- &= \int_{-\infty}^{\infty} \zeta \int_{-(0{\cdot}5 + d_m + x)}^{(0{\cdot}5 + d_m) - x} P_{k+1}^*(\xi, \zeta)\, \mathrm{d}\xi\, \mathrm{d}\xi \\ &= [\sigma_\zeta]_k B_{k+1}^-, \end{aligned} \tag{16}$$

where

$$A_{k+1}^- = \psi_0 + [a_{30}]_{k+1}^- \psi_3 + [a_{40}]_{k+1}^- (\psi_4 - 2\psi_2 + \psi_0) + \cdots, \qquad B_{k+1}^- = \sum_{i=0}^{N} [a_{i1}]_{k+1}^- m_i,$$

and in which

$$\psi_i = d_1^i \exp\left(-\frac{d_1^2}{2}\right) - d_2^i \exp\left(-\frac{d_2^2}{2}\right) \qquad \text{and} \qquad d_{1,2} = \frac{\pm(0{\cdot}5 + d_m) - x_k^-}{\sigma_\xi},$$

$$m_1 = \psi_0, m_2 = \psi_1, m_3 = \psi_2 - \psi_0, m_4 = \psi_3 - 3\psi_1, \ldots.$$

If the iterated operators (7) and (16) are superposed, a mean map (17) for the states before impact to describe the stochastic rattling system has the form

$$\begin{aligned} E[x_\sigma]_{k+1}^- &= x_{k+1}^- + E[\xi]_{k+1}^- = x_{k+1}^- + [\sigma_\xi]_k A_{k+1}^-, \\ E[y_\sigma]_{k+1}^- &= y_{k+1}^- + E[\zeta]_{k+1}^- = \left\{-\varepsilon E[y_\sigma]_k^- - \alpha \cos \tau_k - \frac{\gamma}{\beta}\right\} \exp(-\beta \Delta\tau_k) + \frac{\gamma}{\beta} \\ &\quad + \alpha \cos \tau_{k+1} + (B_{k+1}^- + \varepsilon B_k^- \exp(-\beta \Delta\tau_k))[\sigma_\zeta]_k, \\ \tau_{k+1} &= \tau_k + \Delta\tau_k. \end{aligned} \tag{17}$$

Now the time difference $\Delta\tau_k$ of the two successive impacts can be solved from the following mesh condition of the gears.

$$E[x_\sigma]_{k+1}^- = E[x_\sigma]_k^- \qquad \text{or} \qquad E[x_\sigma]_{k+1}^- = -E[x_\sigma]_k^-.$$

3. RESULTS AND DISCUSSION

In order to understand the study, we look back on the definition of stochastic processes. In 1980, the various stochastic processes were subdivided in reference [16]. One of them was defined as a periodic stochastic process, which had to satisfy the condition that its mean values, variances and correlation were periodic. In 1988, a new stochastic process,

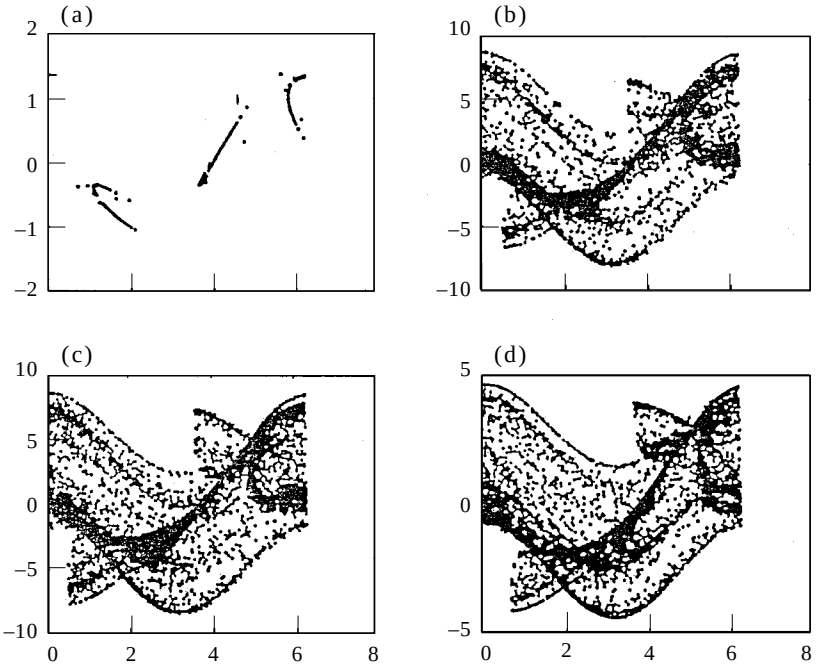

Figure 2. *Poincaré* maps, case 1: (a) dat 11; (b) dat 12; (c) dat 13; (d) dat 14.

called the chaotic stochastic process, was proposed by Kapitaniak [13], who discovered that the probability or the mean value of stochastic process might be chaotic and that phenomenon was defined as random chaos and process as chaotic stochastic process. Based on the above definitions, the chaotic stochastic process can be identified by the mean *Poincaré* map, the power spectrum density and others.

In order to continue the work of references [5, 7–11], data from references [11–14] is used as follows:

dat 11: $\alpha = 0{\cdot}70$, $\beta = 0{\cdot}3$, $\gamma = 0{\cdot}15$ and $\varepsilon = 0{\cdot}7$;

dat 12: $\alpha = 3{\cdot}00$, $\beta = 0{\cdot}1$, $\gamma = 0{\cdot}14$ and $\varepsilon = 0{\cdot}8$;

dat 13: $\alpha = 3{\cdot}00$, $\beta = 0{\cdot}1$, $\gamma = 0{\cdot}10$ and $\varepsilon = 0{\cdot}9$;

dat 14: $\alpha = 1{\cdot}58$, $\beta = 0{\cdot}1$, $\gamma = 0{\cdot}10$ and $\varepsilon = 0{\cdot}9$.

3.1. MEAN POINCARÉ MAPS AND POWER SPECTRA OF MEAN VELOCITY

In this section, two cases are discussed: additional noise; random modulation amplitude.

3.1.1. *Case* 1, $\sigma_1 \neq 0$, $\sigma_2 = 0$

Performing the iterated operator (17) for the above data and the noise intensity $\sigma_1 = \sqrt{\alpha}$, and considering counter meshes of the gears $E[x_\sigma]_{k+1}^- = -E[x_\sigma]_k^-$, the representative calculating results are shown in the following figures. Figures 2(a–d) are mean *Poincaré* maps, in which the horizontal co-ordinate is the time difference $\Delta\tau_k$, and the vertical co-ordinate is the mean velocity before impact $E[y_\sigma]_{k+1}^-$. Figures 2(b–d) display typical chaos and Figure 2(a) shows another structure. That phenomenon can also be observed in the power spectra of mean velocity. Figures 3(a–d) show power spectra in which the horizontal co-ordinate indicates dimensionless frequency f, and the vertical co-ordinate is

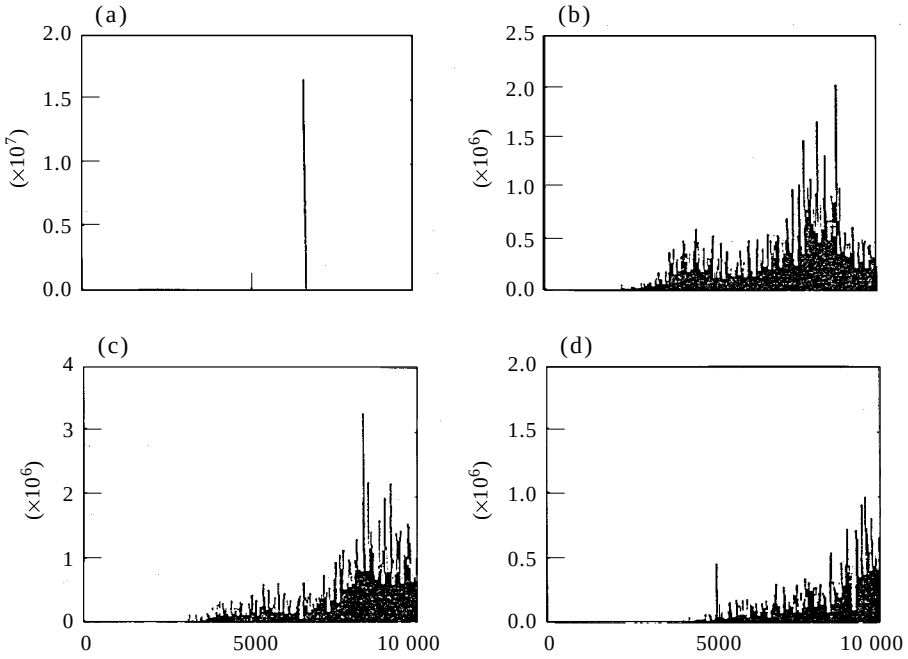

Figure 3. The power spectrum of the mean velocity, case 1: (a) dat 11; (b) dat 12; (c) dat 13; (d) dat 14.

the power spectral density of the mean relative velocity. Whereas all Figures 3(b–d) show wide band spectra, in Figure 3(a), there is only a single peak. It denotes that in counter meshes, for dat 11, the relative velocity is a typical periodic stochastic process, so that Figure 2(a) exhibits no chaotic attractor. A more interesting discovery is that the time difference $\Delta\tau_k$ for dat 14 seems to be a white noise (see Figure 4). In Figure 4, the horizontal co-ordinate indicates dimensionless frequency f, and the vertical co-ordinate is the spectral density of the time difference $\Delta\tau_k$. The various structures in the maps can be understood according to the above descriptions. When the two variables consisting of *Poincaré* maps are wide band processes, the point set of maps nearly fills up a large attraction area of the phase plane. However, when variables are periodic, the point numbers of maps are finite.

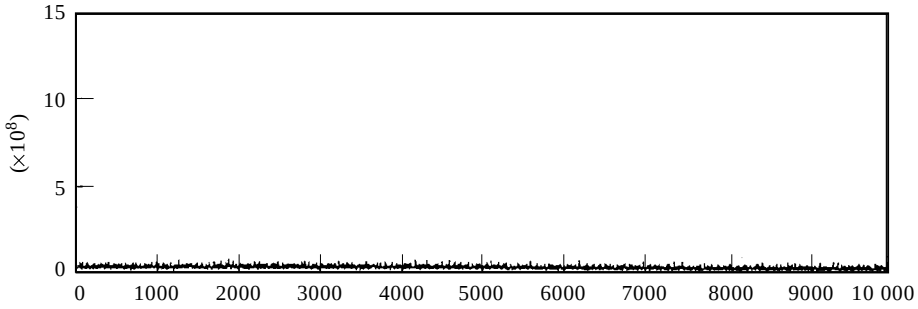

Figure 4. The power spectrum of the time difference, case 1.

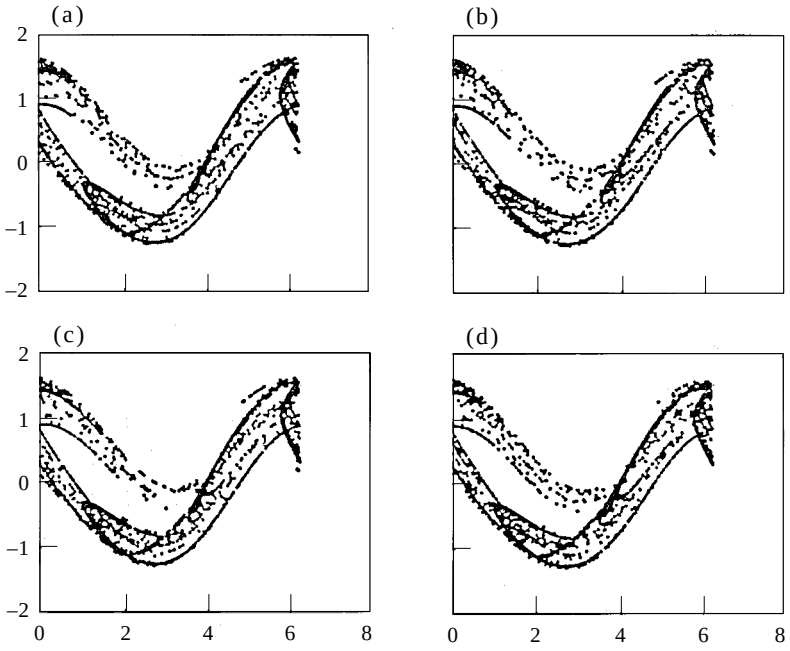

Figure 5. *Poincaré* maps, case 2: $\varepsilon = 0{\cdot}0001$; (b) $\varepsilon = 0{\cdot}001$; (c) $\varepsilon = 0{\cdot}01$; (d) $\varepsilon = 0{\cdot}10$.

3.1.2. *Case* 2, $\sigma_1 = 0$, $\sigma_2 \neq 0$

In this case, the noise intensities are assumed as $\alpha_2 = 0{\cdot}0001$, $\sigma_2 = 0{\cdot}001$, $\sigma_2 = 0{\cdot}01$, $\sigma_2 = 0{\cdot}1$ and dat 11 is used in counter meshes. The mean *Poincaré* maps (See Figure 5), in which the co-ordinates are the same as in Figure 2, show the structure of chaotic attractor. However, this is different from case 1 because the point set of maps does not fill up the attraction areas. This phenomenon can also be observed in Figure 6 which gives power spectra of mean velocity. Figures 6(a–d) exhibit continuous spectra, but which possesses narrow-band character. This phenomenon may be interpreted as follows: in the case of random modulation amplitude, only the excitation amplitude is randomly modulated and the frequency fluctuates around a principal frequency; thus the mean velocity is narrow-band process. Moreover, it is interesting that the power spectral densities do not always improve as the intensity of the external noise σ_2 increases. In Figure 6(b) ($\sigma_2 = 0{\cdot}001$), the frequency band is wider and the peaks of the spectral density of mean velocity are lower than others in Figure 6. This phenomenon leads to a new idea that one can control rattling noise by external noise.

3.2. CHARACTERISTIC FUNCTION

In this section, case 1 only is considered. Reference [10] has shown that the probability distribution can be used to characterize the fluctuations of the total energy of the system. In reference [13], a chaotic stochastic process was defined through the probability density. The probability possesses intersting behaviour and can be used to study the chaotic phenomena. In the present paper, a non-Gaussian closure technique is adopted and thus it is inevitable that the probability can satisfy the bifurcation condition according to its definition in reference [13]. However, it is difficult to determine whether the probability density possesses the structure of a Cantor set. Therefore, instead of the probability density, a characteristic function such as Fourier transform of the PDF is used to detect

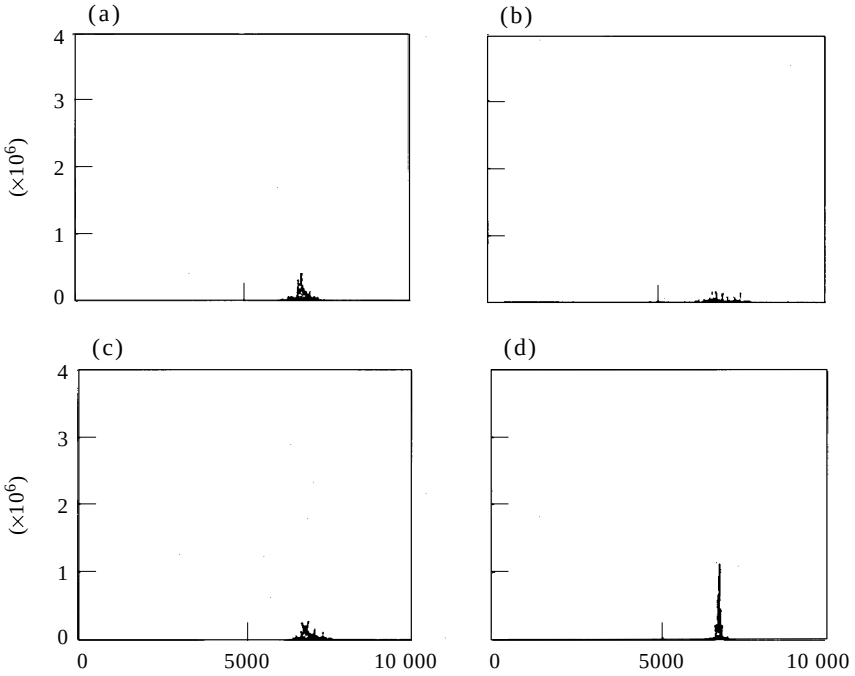

Figure 6. The power spectrum of the mean velocity, case 2: (a) $\varepsilon = 0{\cdot}0001$; (b) $\varepsilon = 0{\cdot}001$; (c) $\varepsilon = 0{\cdot}01$; (d) $\varepsilon = 0{\cdot}1$.

the chaotic stochastic behaviour of the system. The results show that the characteristic function can exhibit typical chaotic attractor. Figure 7 gives the information of the imaginary part of the characteristic function $F(\vartheta)$ of the mean velocity in which the horizontal co-ordinate indicates the imaginary part of the characteristic function before the kth impact $[\mathrm{Im}\,(F(\vartheta)]_k^-$ and the vertical co-ordinate is one before the $k+1$th $[\mathrm{Im}\,(F(\vartheta)]_{k+1}^-$. For $\vartheta = 2$, dat 11, in counter meshes, Figure 7(a), for $\alpha = 0{\cdot}7$, shows a periodic stochastic motion and Figure 7(b), for $\alpha = 0{\cdot}85$, shows a chaotic stochastic motion. It is significant that the imaginary part of the characteristic function can display the same structure as mean *Poincaré* maps in Figure 2, and so a characteristic function is suggested to detect the random chaos.

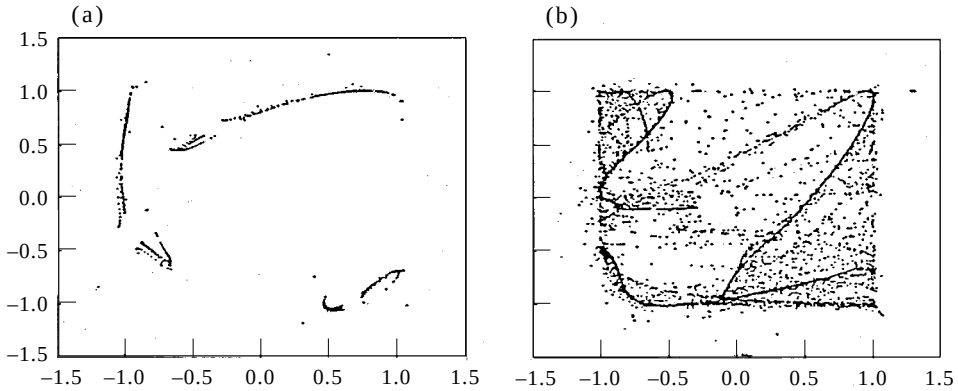

Figure 7. The imaginary part of the characteristic function, case 1: (a) $\alpha = 0{\cdot}7$; (b) $\alpha = 0{\cdot}85$.

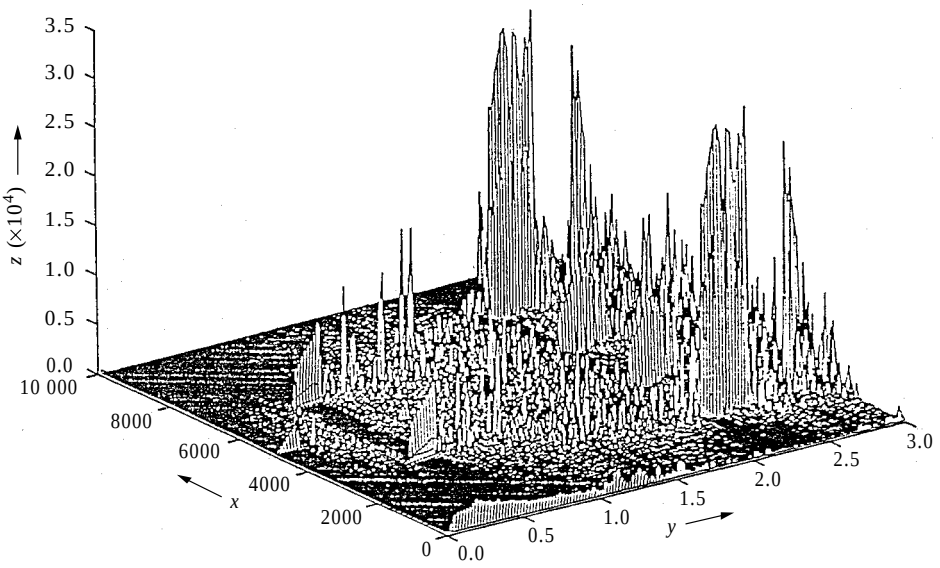

Figure 8. The bifurcation diagram in the frequency domain, case 1.

3.3. ROUTE TO RANDOM CHAOS

The above section shows that the mean relative velocity is a most interesting physical magnitude, which can display various motions if the system parameters change. In this section, a bifurcation diagram in the frequency domain is developed and the routes to random chaos are compared, using date 11, in counter meshes and assuming the noise intensity $\sigma_1 = \sigma_2 = \sqrt{\alpha}$.

3.3.4. *Case* 1, $\sigma_1 \neq 0$, $\sigma_2 = 0$

The computed results in Figure 8 show that the x co-ordinate designates dimensionless frequency f, the y co-ordinate denotes the excitation amplitude α, and z stands for the power spectrum density of the mean velocity. Compared with the deterministic chaos in [11], the analogous behaviour is that the route to random chaos also goes through a sequence of period–doubling bifurcation and intermittence, and the difference is that the frequency does not appear in a single form, but in small block. In Figure 8, one can see only a small frequency block in the domain $\alpha = 0{\cdot}0$–$0{\cdot}15$. When $\alpha = 0{\cdot}13$–$0{\cdot}3$, the diagram shows an intermittence of chaos. In the domain $\alpha = 0{\cdot}3$–$0{\cdot}6$, two small blocks bifurcate. Then an intermittence of chaos occurs in the domain $\alpha = 0{\cdot}6$–$2{\cdot}0$. When $\alpha = 2{\cdot}0$–$2{\cdot}4$, the diagram is split into four small blocks, and so, on, until at last it tends to random chaos. The frequency distribution in the diagram is not very regular. Some smaller peaks exist in the neighbourhood of the principal frequency blocks, which is different from the deterministic case.

3.3.2. *Case* 2, $\sigma_1 = 0$, $\sigma_2 \neq 0$

Now the case of random modulation is discussed. Figure 9 is also a bifurcation diagram in the frequency domain. Comparing the two diagrams in Figures 8 and 9, it is found that two routes are different. In the additional noise case 1, the route to random chaos is relatively regular through a sequence of periodic-doubling bifurcation and intermittence,

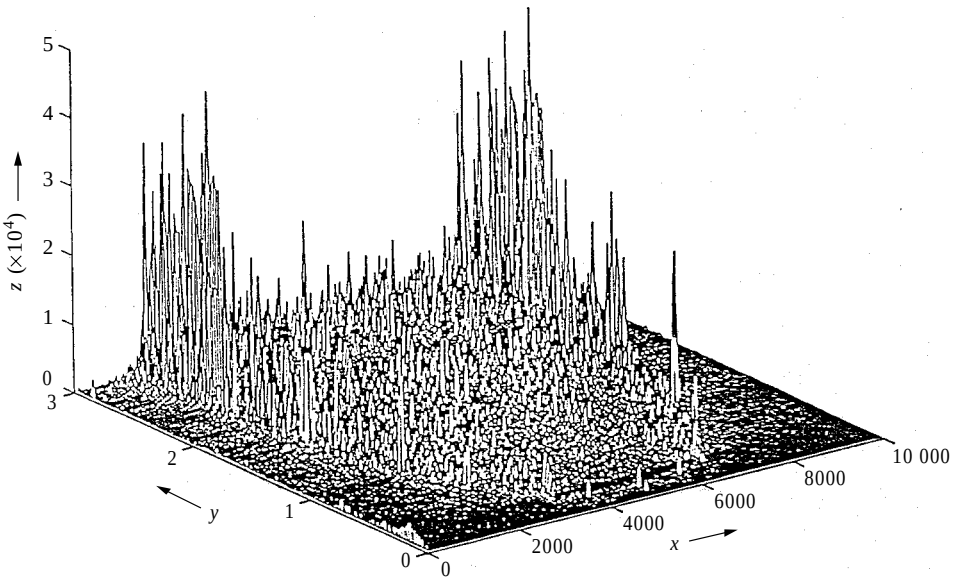

Figure 9. The bifurcation diagram in the frequency domain, case 2.

but in the random modulated case 2, the sequence of periodic-doubling bifurcation is not evident. It seems that there is "chaos" everywhere in Figure 9. That phenomenon reveals that the random modulated rattling system is obviously more complex than the one with additional noise. By the use of a bifurcation diagram in the frequency domain, the influence of external disturbance on a non-linear system in energy can be examined and a chaotic region can be determined.

4. CONCLUSIONS

In the present paper, a discrete stochastic model described by a mean map has been established from a real vibrating system and the random chaos on the dynamcis of a rattling system has been explored. It is a very specific problem, however. Based on our study the existence of the random chaos has been justified. More broadly, this investigation method can be used in more general discussion of other systems.

In our study, the mean *Poincaré* map, the power spectrum density and the characteristic function have been investigated for the dynamics of random chaos. The calculation results have shown that the mean *Poincaré* maps exhibit clearly typical chaos and the power spectra of mean velocity display the behaviour of a continuous spectrum. The characteristic function of mean velocity has shown the same structure as a *Poincaré* map. Moreover, it has been detected that the time difference may be a white noise. Those phenomena can be iterated so that the random chaos can occur in some real physical systems. It is well known that rattling vibration causes noise and its deterministic model is only an ideal one, so that based on the present work, the use of a stochastic model described by a mean map is suggested to investigate rattling noise.

The final conclusion is that the rattling system studied here, as an impulsive system, is extremely convenient for detailed investigation of complex phenomena. The routes to random chaos have shown that the chaotic stochastic vibration can be controlled by variation of a single system parameter. It is very important in practice to reduce the rattling noise. For the random modulated system, the possibility of reducing noise by noise has been found, and continuing work for such a system is suggested.

REFERENCES

1. F. KÜCÜKAY 1987 *Dynamik der Zahnradgetrieb*, *Modell*, *Verfahren*, *Verhalten*. Berlin–Heidelberg: Springer Verlag.
2. F. KÜCÜKAY and F. PFEIFFER, 1986 *Ing-Archiv* **56**, 25–37. Ueber Rassel in Kfz-Schaltgetrieben.
3. F. PFEIFFER 1984 *Ing-Archiv* **54**, 232–240. Mechanische System mit unstetigen Uebergaengen.
4. F. PFEIFFER 1987 *Proceedings of the 7th World Congress on the Theory of Machines and Mechanisms*, *Sevilla*. On steady dynamics in machines with plays.
5. F. PFEIFFER 1988 *Ing-Archiv* **58**, 113–125. Seltsame Attraktoren in Zahnradgetrieben.
6. C. F. MOON 1987 *Chaotic Vibration*. New York: John Wiley and Sons.
7. K. KARAGIANNIS 1989 *VDI-Bericht Nr*. 125. Analyze stossbehafteter Schwigungssysteme mit Anwendung auf Resselschwingungen in Getrieben.
8. K. KARAGIANNIS and F. PFEIFFER 1991 *Nonlinear Dynamics* **2**, 367–387. Theoretical and experimental investigations of gear-rattling.
9. F. PFEIFFER and A. KUNERT 1990 *Nonlinear Dynamics* **1**, 63–74. Rattling models from deterministic to stochastic processes.
10. A. KUNERT and F. PFEIFFER 1991 *Nonlinear Dynamics* **2**, 291–304. Description of chaotic motion by an invariant probability density.
11. A. KUNERT 1992 *VDI-Bericht Nr*. 175. Dynamik spielbehafter Maschinenteile.
12. F. MOSS and P. V. E. MCVLINTOCK 1985 *Noise in Nonlinear Dynamical Systems*, Volume 2. Cambridge: Cambridge University Press.
13. T. KAPITANIAK 1988 *Chaos in System with Noise*. Singapore: World Scientific.
14. R. A. IBRAHIM, 1985 *Parametric Random Vibration*. New York: John Wiley and Sons.
15. S. H. CRANDALL 1985 *International Journal of Non-linear Mechanics* **20**, 1–8. Non-Gaussian closure techniques for stationary random vibration.
16. R. Z. HAŚMINISKIĬ 1980 *Stochastic Stability of Differential Equations*. U.S.A.: Sijloff Noordhoff.

APPENDIX: NOMENCLATURE

R_e and R_1	basic radii
$e(t)$	harmonic rotation
a	amplitude
ω	frequency
v_1	constant play in mesh plane
I_1	inertia moment of driven gear wheel
ϕ_1	angular displacement
T_1	constant moment
d_1	damping ratio in free flight phase
ε	coefficient of restitution
x	relative velocity displacement of unperturbed system
y	relative of unperturbed system
β	damping ratio in free flight phase
γ	indicates constant moment
τ	dimensionless time
α	excitation amplitude
x_σ	relative displacement of perturbed system
y_σ	relative velocity of perturbed system
$\sigma_i (i = 1, 2)$	intensity of random forces
$\eta(\tau)$	standard Gaussian white noise
ξ and ζ	stochastic variables
$P^*(\xi, \zeta)$	non-Gaussian probability distribution
$\rho_{\xi\zeta}$	correlation coefficient of the random variables ξ and ζ
λ_{np}	moments
$P(\xi, \zeta)$	standard Gaussian normal distribution
$\sigma_i (i = \xi, \zeta)$	standard derivations
$m_i (i = \xi, \zeta)$	mean values
$F(\vartheta)$	characteristic function